IOP Conf. Series: Materials Science and Engineering **158** (2016) 012064 doi:10.1088/1757-899X/158/1/012064

Detached eddy simulations of side-loads in an overexpanded nozzle flow

E A Luchikhina and L E Tonkov

Institute of Mechanics Ural Branch of the Russian Academy of Sciences, ul. T. Baramzinoy, 34, Izhevsk, 426067, Russia

E-mail: tnk@udman.ru

Abstract. In this paper, we numerically examine the separated flow in an overexpanded nozzle developed during the starting phase of a rocket engine featuring the side-load effect. We use detached eddy simulation and compare our results with the existing experimental data. The calculations are based on finite volume approximation of the Navier-Stokes equations for perfect gas and pressure-based formulation with PISO coupling. The main flow properties (wall pressure levels, shock waves pattern, side load locus) are rather well reproduced. We suggest using a delayed detached eddy simulation for more accurate predictions of the flow separation.

1. Introduction

The loss of axial symmetry of a supersonic nozzle flow and, as a result, the lateral deviation of the thrust vector is inherent in any real flow. However, for a number of applications, such as first-stage rocket engines with high geometric expansion ratio of the nozzle, the loss of symmetry results in significant transient side loads. The side-load assessment is a challenging engineering problem. The side load effect has been studied for American (J-2, J-2S, J-2X), European (Vulcain), and Japanese (LE-7A) engines [1].

The start-up of a rocket engine nozzle that operates in overexpanded flow conditions is not just an important practical problem. It is interesting in terms of developing new mathematical models and numerical schemes. This class of flows has a number of specific features, such as: sub- and supersonic flow regions separated by shock waves pattern, recirculation bubble with boundary layer detachment, and reattachment on the nozzle wall. Shock-induced separation flow caused by these features plays a key role in the loss of symmetry and the side-load effect [2]. Therefore, for accurate numerical modeling of the internal gas dynamics of the nozzle, it is necessary to take into account all these processes.

On the numerical side, most research on shock patterns and side-loads in rocket nozzle with high area-ratio is based on the resolution of the Unsteady Reynolds Averaged Navier–Stokes equations (U-RANS) in conjunction with k-ω family of turbulence models [2,3,4,5]. There are very few works on using Large-Eddy Simulation (LES) to study side-loads effect in an overexpanded nozzle flow. A detailed description of the numerical experiment based on the RANS–LES method, namely Delayed Detached Eddy Simulation (DDES), can be found in [6].

It is well known that the solving RANS equations requires less computing resources, but RANS-based models are not universal, which limit their applicability in practice. Furthermore, RANS time averaging may be unsuitable for solving significantly transient problems.

Direct numerical simulation (DNS) is still difficult because of the high computational costs and its applications is limited to a small set of model examples. An alternative to DNS is eddy-resolving methods (LES, DES), which are based on the idea of spatial low-pass filtering of the original system of equations (1). Such filtering reduces the computational cost by ignoring the smallest length scales, which are the most computationally expensive to resolve. However, when considering the near-wall flows, the computational cost dramatically increases, since significant turbulence eddy structures near the wall are quite small, which in turn leads to a filter width decrease.

Detached Eddy Simulation (DES) is a promising approach to modeling the turbulent flows. In this method, “simple”" RANS-based turbulence model, for example Spalart–Allmaras (SA) model, is used for simulation of only structures with dimensions the smaller size of the filter, and larger eddies are resolved exactly.

The aim of this work is to investigate the special regime and side-loads effect using advanced DES turbulence modeling approaches.

This paper is structured as follows. Section 2 describes the computational fluid dynamics model and grid. Section 3 introduces DES-SA turbulence model in the frame of overexpanded nozzle flows. Section 4 then presents the summary of results obtained and their analysis. Section 5 concludes the paper.

2. Mathematical model and computational methodology

The computational fluid dynamics model is based on a multi-dimensional system of Navier–Stokes equations for perfect gas:

$$\begin{aligned} &\partial\rho/\,\partial t + \nabla\cdot\rho\mathbf{U} = 0,\\ &\partial\rho\mathbf{U}/\,\partial t + \nabla\cdot\rho\mathbf{U}\mathbf{U} = -\nabla p + \nabla\boldsymbol{\sigma},\\ &\partial\rho E/\,\partial t + \nabla\cdot\rho\mathbf{U}E = -p(\nabla\cdot\mathbf{U}) - \nabla\cdot\mathbf{q} - \nabla\cdot(\boldsymbol{\sigma}\cdot\nabla\mathbf{U}). \end{aligned} \tag{1}$$

Here $\boldsymbol{\sigma}$ — viscosity stress tensor, $E = \frac{1}{2}\mathbf{U}^2 + c_v T$ — total energy, $\mathbf{q}$ — heat flow.

Computational domain covers the nozzle interior as well as the freestream region. Following [4], the geometric parameters of the nozzle (J-2S) were selected following: length of diverging section $l = 1.913$ m, throat radius $r_* = 0.154$ m, exit radius $r_a = 0.975$ m.

Computational block-structured grid was generated by rotating an 2-D grid (pic. 1) around the symmetry axis to become a three-dimensional grid containing 4 552 500 hexagonal cells. Let us note that the final 3-D grid is symmetric to the central axis, ensuring that the computed asymmetric flow comes from the physics and not an asymmetric grid topology.

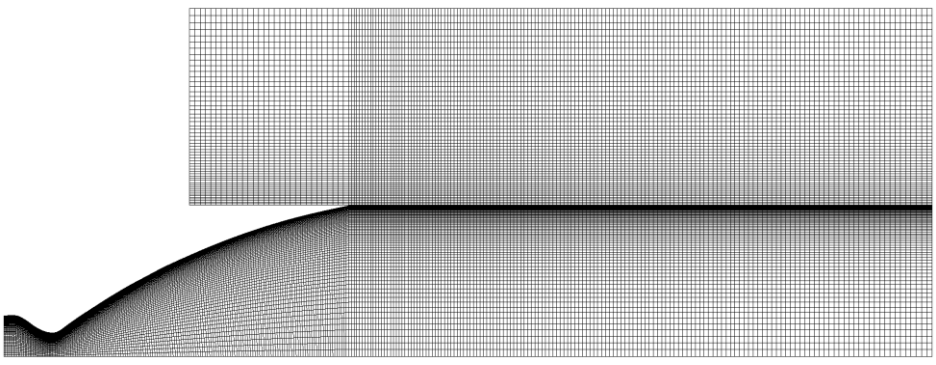

Figure 1. 2-D grid used to construct the final axisymmetric 3-D grid

No-slip and adiabatic boundary conditions are imposed on all the nozzle walls. The outlet boundary condition was set to the fixed-pressure type with ambient pressure $p_a = 10^5$ Pa. The inlet boundary condition was set to the total-pressure type with stagnation pressure $p_* = 43 \cdot 10^5$ Pa.

At walls, the modified turbulent kinematic viscosity $\tilde{\nu}$ was set to zero, at inlet boundary — $\tilde{\nu} \approx \nu$ [7]. Initial conditions was established by stagnation values into combustion chamber: $U_s = 0$, $p_s = 43 \cdot 10^5$ Pa, $T_s = 300$ K, and ambient values behind throat: $U_a = 0$, $p_a = 1 \cdot 10^5$ Pa, $T_a = 288$ K.

The calculations is based on finite volume approximation of system (1) and pressure-based formulation with PISO coupling. A second-order central-difference scheme was employed to discretize the diffusion fluxes and source terms. For the convective terms, a second-order, total-variation-diminishing, upwind-difference based scheme with Van Leer limiter function was used. The numerical scheme provides a good approximation and stability in the calculation of sub- and supersonic flows, containing shock-wave discontinuities for the wide range of Mach numbers.

3. Turbulence modelling: detached eddy simulation

The nature of the investigated flow is influenced by large eddies behind the Mach disk as well as small eddies in wall-near recirculation zones. In the frame of DES, the grid resolution requirements in the boundary layer are closer to those of RANS, thereby significantly reducing the computational cost. At the same time a DES is an LES outside the boundary layer, that allows as to resolve a turbulence structures on wide-range scales without a time averaging of (1).

From the computational point of view, the notation of RANS and LES governing equations just the same and the RANS model can be reduced to a LES subgrid-scale one by replacing the linear scale in a destruction term for the eddy viscosity. Thus, the computational model, based on the system of Navier–Stokes equations (1), includes one additional transport equation for modified eddy viscosity $\tilde{\nu}$ [8]:

$$\frac{\partial \tilde{\nu}}{\partial t} + \mathbf{U} \cdot \nabla \tilde{\nu} = \frac{1}{\sigma}\{\nabla[(\nu + \tilde{\nu})\nabla\tilde{\nu}] + c_{b2}\nabla\tilde{\nu} \cdot \nabla\tilde{\nu}\} + S. \quad (2)$$

Generation term in equation (2) defined by:

$$S = c_{b1}\tilde{S}\tilde{\nu} - c_{w1}f_w\left(\frac{\tilde{\nu}}{d}\right)^2, \quad (3)$$

where d is the linear scale of turbulence.

Relation between modified eddy viscosity and turbulence viscosity are given by: $\nu_t = f_{v1}\tilde{\nu}$ or $\mu_t = \rho f_{v1}\tilde{\nu}$.

The above formulation of the Spalart–Allmaras (SA) model (2)-(3) does not include the terms for realisation of a numerical-induced laminar-turbulent transition [7]. The values of constants and functions can be found, for example, in [8]. In order to use SA model as a LES subgrid-scale one is necessary to replace the linear scale d by

$$l_{\mathrm{DES}} = \min\{l_{\mathrm{RANS}}, C_{\mathrm{DES}}\Delta\}, \quad (4)$$

where l_{RANS} is closest wall distance, $\Delta = \sqrt[3]{\Delta_x\Delta_y\Delta_z}$ — LES filters width and $C_{\mathrm{DES}} = 0.65$.

4. Results and discussion

Following [4], we have considered the time interval $0 \le t \le 0.1818$ s which is a period sufficiently long to generate restricted shock separation (RSS) flow mode then transition to free shock separation (FSS) flow with near-wall recirculation zones.

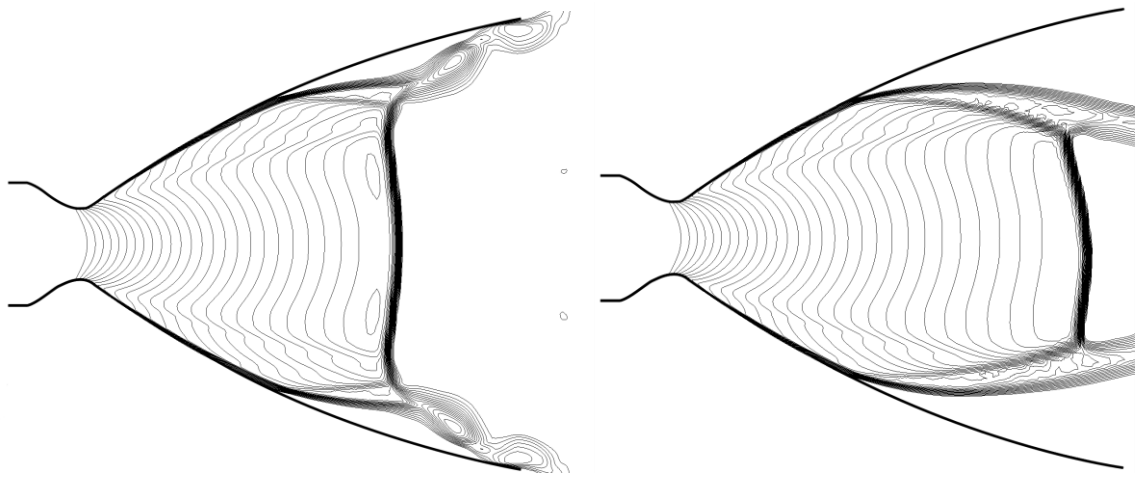

(a) (b)

Figure 2. The iso-Mach contour lines: a) $t = 0.007$s; b) $t = 0.186$s.

The iso-Mach contour lines at two time slices $t = 0.007$ s and $t = 0.186$ s are given in figure 2. One can notice loss of symmetry (figure 2, b), due to the instability of the flow in recirculation zone.

Computed by DES-SA model (1), (2)–(3) side load locus are plotted in figure 3, b versus numerical results [4] (figure 3, a). As seen in the plots, the present data are in good agreement with [4], but oscillation frequency is a slightly higher.

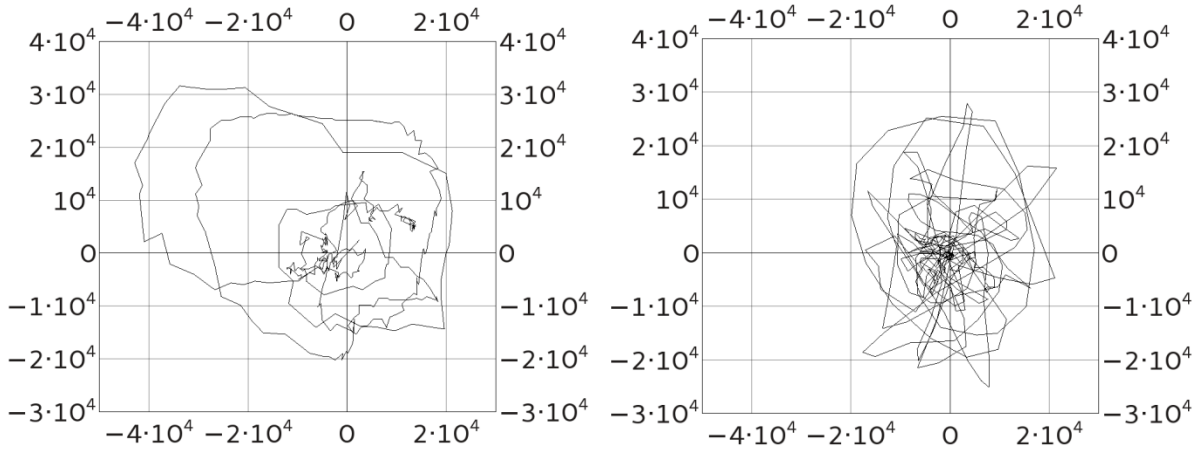

(a) (b)

Figure 3. Computed side force locus F_{xy}, N: a) numerical data [4]; b) present calculations by DES-SA model.

Figure 4 shows in comparison with [4] computed streamwise wall pressure distributions for FSS mode (a) and RSS mode (b).

The vertical lines on the plot show the set of wall pressure values in the corresponding cross-sestion and their magnitude indicating the flow is mostly asymmetric. It can also be seen that the side load effect develops at FSS mode. Examining the wall pressure distributions in figure 4, it can be seen that a calculated flow separation point located somewhat upstream than that of [4], and the maximum

pressure value slightly higher. From the results it is concluded that the subgrid-scale eddy viscosity model needs to be adjusted as well as computational grid.

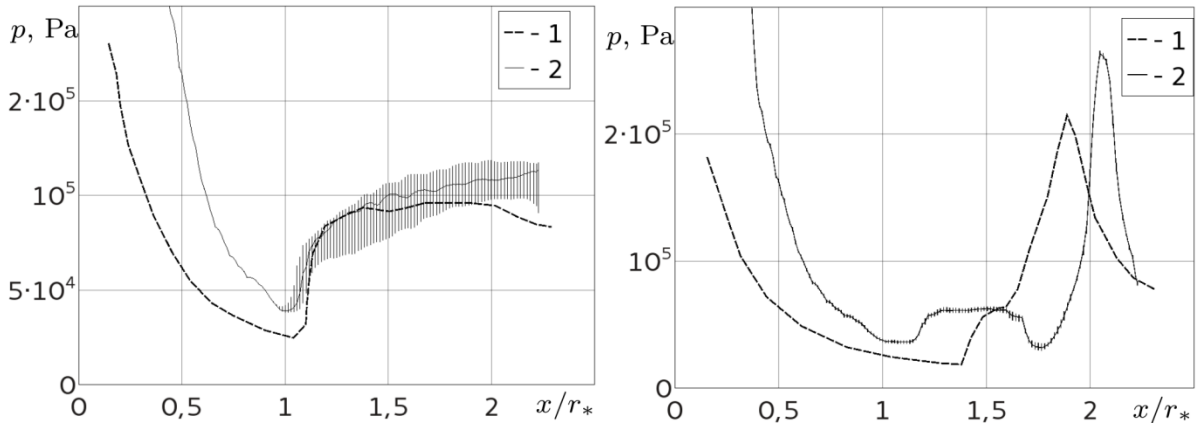

(a) (b)

Figure 4. Computed streamwise wall pressure distributions, FSS flow mode (a); RSS flow mode (b): 1 — numerical data [4]; 2 — present calculations by DES-SA model; a) $t = 0.186$ b) $t = 0.007$.

5. Conclusions

The nozzle flow developed during the starting phase of the rocket engine was analyzed via numerical simulation using detached eddy approach (DES) in conjuncton with the Spalart–Allmaras eddy viscosity model; the results was compared with data [4]. The comparative study provide some evidence for the correctness of the mathematical model that adequately describes the main characters of this type of flows. The resulting differences indicate that additional work is needed to improve the method and computational grid resolution first of all at near-wall zone.

It is suggested that a delayed DES (DDES) approach should be used for more accurate predictions of the separation point position. Furthermore, it is necessary that a more thorough study of the eddy viscosity model parameters that are responsible for the generation-destruction balance at RANS/LES crossover region.

Acknowledgments

This work was supported in part by the RFBR under grants 14-08-00064-a and 14-01-00055-a.

References

[1] Tomita T, Sakamoto H, Onodera T, Sasaki M, Takahashi M and Tamura H 2004 *AIAA Paper* **4** 9
[2] Glushko G S, Ivanov I E and Kriukov I A 2010 *Physical and Chemical Processes In Gas Dynamics* **1** 172–179
[3] Wang T S 2009 *Shock Waves* **19** 251–264
[4] Zhao X, Bayyuk S and Zhang S 2013 Aeroelastic response of rocket nozzles to asymmetric thrust loading *Computers and Fluids* 76 pp 128–148
[5] Kuzmin I, Tonkov L and Chernova A 2015 Izv. *Inst. Mat. Inform., Udmurt. Gos. Univ.* **2(46)** 93–98
[6] Deck S 2009 *Shock Waves* **19** 239–249
[7] Garbaruk A V, Niculin D, Strelets M K, Dyadkin A, Krylov A and Stekenius K 2013 *Progress in Flight Physics* **5** 3–22
[8] Spalart P R and Allmaras S R 1994 A *La Recherche Aerospatiale* **1** 5–21